The SZ Effect as a Probe of Non-Gravitational Entropy in Groups and Clusters of Galaxies

A. Cavaliere[1] and N. Menci[2]
[1] Astrofisica, Dip. Fisica 2a Università, Roma I-00133
[2] Osservatorio Astronomico di Roma, Monteporzio, I-00044

ABSTRACT

We investigate how strongly and at what scales the Sunyaev-Zel'dovich effect reflects the shifting balance between two processes that compete for governing the density and the thermodynamic state of the hot intra-cluster medium pervading clusters and groups of galaxies. One such process is the hierarchical clustering of the DM; this induces gravitational heating of the diffuse baryons, and strives to push not only the galaxy systems but also the ICM they contain toward self-similarity. Away from it drives the other process, constituted by non-gravitational energy fed back into the ICM by the condensing baryons. We base on a semi-analytic model of galaxy formation and clustering to describe how the baryons are partitioned among the hot, the cool and the stellar phase; the partition shifts as the galaxies cluster hierarchically, and as feedback processes (here we focus on stellar winds and Supernova explosions) follow the star formation. Such processes provide a moderate feedback, whose impact is amplified by the same large scale accretion shocks that thermalize the gravitational energy of gas falling into the growing potential wells. We use the model to compute the Compton parameter y that governs the amplitude of the SZ effect, and to predict how this is affected by the feedback; for individual clusters and groups we find a relation of y with the ICM temperature, the $y-T$ relation, which departs from the form suggested by the self-similar scaling, and bends down at temperatures typical of galaxy groups. We also compute the average $\langle y\rangle$ and the source counts as a function of y under different assumptions concerning feedback strength and cosmology/cosmogony. We then discuss to what extent our results are generic of the hierarchical models of galaxy formation and clustering; we show how the $y-T$ relation, to be measured at μwave or sub-mm wavelengths, is model-independently related to the shape of the $L-T$ correlation measured in X-rays. We conclude that these observables together – because of their complementarity and their observational independence – can firmly bound the processes responsible for non-gravitational entropy injections into the ICM.

Subject headings: galaxies, formation - galaxies: groups, clusters - X-rays: galaxies, clusters

1. Introduction

The evolution of galaxies and galaxy systems may be understoood in terms of a competition between two processes. One is the dominant gravitational drive of the dark matter (DM) that leads to hierarchical clustering; this builds up "haloes" that grow larger and deeper by the merging of smaller clumps (see Peebles 1993), and yet remain closely *self-similar*, i.e., with central densities and profiles which are nearly scaled versions of each other (see Navarro et al. 1995). The other process is the active *response* of the baryons contained in such potential wells; this strives to drive the radiative structures *away* from self-similarity.

Groups and clusters of galaxies provide an ideal testing ground for such a picture. On the one hand, their deep gravitational wells are dominated by DM masses ranging from $M \approx 10^{13}$ to $10^{15}\ M_\odot$. Their sizes may be defined by the virial radius R where the DM density ρ at formation exceeds by a factor of about $2\,10^2$ the background value $\rho_u(z) \propto (1+z)^3$; they scale as $R \propto (M/\rho_u)^{1/3}$, and match or exceed $R \sim 1.5\,h^{-1}$ Mpc for the rich clusters. The well depths may be measured in terms of the circular velocities $v = (G\,M/R)^{1/2} \propto M^{1/3}\rho_u^{1/6}$, which attain or exceed 1400 km s^{-1} in rich clusters today.

On the other hand, such wells also contain large masses of diffuse baryons, of order $M_b \approx 0.15\,M$ (White et al. 1993; White & Fabian 1995; Fukugita, Hogan & Peebles 1998); these are in the state of a hot plasma, the intra-cluster medium or ICM.

Its temperatures may be estimated on assuming also the ICM to be in virial equilibrium; this provides the scaling $kT \approx kT_V \propto v^2$, and values in the range $kT \sim 0.5 \div 10$ keV in going from poor groups to rich clusters. By and large, these results are confirmed by the observations of many high-excitation lines at keV energies and of the X-ray continuum.

In fact, the ICM is well observable at X-ray energies through its thermal bremsstrahlung emission $L \propto n^2\,T^{1/2}\,R^3$, which from groups to rich clusters ranges from 10^{42} to several 10^{45} erg s^{-1} for typical densities $n \sim 10^{-(3\pm1)}$ cm^{-3}.

But the same hot electrons also inverse-Compton upscatter the photons of the CMB, and thus they tilt slightly the black-body spectrum toward higher energies; at microwave wavelengths the result toward individual clusters is an apparent intensity

decrement $\Delta I/I \approx -2\,y$ in terms of the Compton parameter $y \propto n\,kT\,R$. Numerical values $|\Delta I/I| \sim 10^{-4}$ had been predicted by Sunyaev & Zel'dovich (1972) (hence the acronym SZ effect), and are being measured in a growing number of rich clusters; for reviews and recent data, see Rephaeli (1995), Birkinshaw (1999), Carlstrom et al. (2000), Saunders & Jones (2000). The computation of y and of related observables from a comprehensive model for the thermal state of the ICM constitutes the main scope of the present paper; its plan is as follows. In §2 we discuss how the SZ probe fits into the current debate concerning the role of non-gravitational processes in setting the thermal state of the ICM. In §3 we describe how we compute such state, and how our model fits into the current efforts toward including star formation and other baryonic processes in the hierarchical clustering picture; at the end of the section we show how the SZ observables are computed on the basis of our specific model. In §4 we present our results and predictions concerning the $y - T$ relation and the integrated SZ observables, namely, the source counts and the average Compton parameter $\langle y \rangle$. In §5 we discuss the building blocks of our model, and make contact with other related works; we also stress the generic aspects of the link between the $y - T$ and the $L - T$ relations. In the final §6 we summarize our predictions and conclusions.

2. The State of the ICM

Before we embark into technical issues, we discuss the framework of observations and theories in which the present work is to fit.

2.1. The self-similar picture

The simplest picture of the ICM would have its thermal energy to be of purely gravitational origin; that is to say, originated only by gravitational energy released on large scales comparable with R as the external gas falls into the self-similar potential wells provided by the DM (Kaiser 1986), and thermalized by some effective coupling. By itself, the process would establish temperatures $T \approx T_V$ and produce self-similar ICM distributions in the wells, with central densities n just proportional to the DM density ρ, hence to the external ρ_u. If so, the DM scaling recast into the form $R \propto T_V^{1/2}\,\rho^{-1/2}$ easily yields that the resulting X-ray luminosity should scale as

$$L_{grav} \propto \rho_u^{1/2}\,T_V^2. \tag{1}$$

However, this simple picture is challenged – especially at the scales from poor clusters to groups of galaxies – by several recent X-ray observations.

2.2. Broken self-similarity

First, the observed shape of the $L - T$ correlation departs from $L \propto T^2$ and bends down progressively in moving from very rich clusters down to poor groups (see Ponman et al. 1996; Helsdon & Ponman 2000), as if lower T should imply considerably lower values of n and thus much lower luminosities L. Second, the profiles of the X-ray surface brightness do not appear to be self-similar, rather they flatten out at low T (Ponman, Cannon & Navarro 1999). Third, the X-ray luminosity function $N(L, z)$ shows little or no evidence of cosmological evolution (Rosati et al. 1998); if anything, weak negative evolution may affect the bright end of the LFs, but surely the data rule out the strong, positive "density evolution" that would prevail if the relation $n \propto \rho$ held and kept $L(z)$ roughly constant.

All that points toward an ICM history more complex than pure, gravitational heating from infall into the forming DM potential wells, as already realized by Kaiser (1991). It rather suggests additional heating by injection of some non-gravitational energy, which ought to be more important for the shallower wells of the groups to the point of breaking there the simple assumption $n \propto \rho$.

To single out the baryonic processes responsible for this, it is clearly useful (see Cavaliere 1980, and Bower 1997) to consider the ICM specific entropy (in Boltzmann units) $S = ln\, p/n^{5/3} \propto ln\, kT/n^{2/3}$, the one combination of T and n that is invariant under pure adiabatic compressions of the gas falling into the wells. Data and N-body simulations (Lloyd-Davies, Ponman & Cannon 1999) concur to show that in moving from clusters to groups this quantity is far from behaving in the way suggested by the self-similar scaling

$$S_{grav} \propto ln\, T_V\, \rho_u^{-2/3} \ . \tag{2}$$

In fact, when the values averaged out to $10^{-1}\, R$ are plotted as a function of T, they level off to a "floor" corresponding to $e^S \propto kT/n^{2/3} \approx 100$ keV cm^2. On the other hand, in clusters S as a function of r increases outwards (see Lloyd-Davies, Ponman & Cannon 1999). These behaviours indicate that the entropy is enhanced in two ways relative to the self-similar scaling, both in the present groups and during the history of the clusters.

2.3. Non-gravitational processes

One promising explanation of all these observational features goes back to heating/ejection of the ICM by thermal/mechanical feedback effects from star formation during the process of galaxy build up and clustering into groups (Cavaliere, Menci & Tozzi 1997, 1999; Wu, Fabian & Nulsen 1998; Valageas & Silk 2000; Fujita & Takahara 2000).

We shall adopt as a baseline the injections of momentum and of thermal energy contributed both by stellar winds (Bressan, Chiosi & Fagotto 1994) and by Type II Supernovae (SN) that follow the formation of massive stars in shallow wells. The latter include not only the current groups, but also the progenitors of current clusters; in fact, the hierarchical clustering paradigm envisages such events to take place also during the early phase of a cluster's history when the progenitors were just groups, which subsequently grew by the progressive inclusion of additional mass lumps of comparable or smaller sizes.

Such combined feadback effects naturally imply the ICM to be not only pre-heated to about $0.2 \div 0.3$ keV, but also to be dynamically ejected outwards to the perifery of the DM haloes, at low densities $n \sim 10^{-4}$ cm^{-3}. This is how a relatively high entropy level corresponding to $kT/n^{2/3} \sim 10^2$ keV cm^2 may be attained in groups as well as in the central regions of the forming clusters. In the latter, the subsequent evolution will include adiabatic compression of the gas accreted along with the DM into the deepening wells (Tozzi & Norman 2000), a process that conserves entropy. But the gas falling supersonically into such deep potential wells will also pass through strong accretion shocks at about the virial radius R, the process whereby the ICM is actually heated to the current high temperatures of order T_V. By the same token, much additional entropy is deposited in the outer regions, corresponding to shock conversion of the bulk inflows $v_1 \approx v$ into thermal energy.

This scenario leads one to expect in the groups not only lower densities, and much lower bremsstrahlung emission compared with the scaling $L \propto T^2$, as observed; but it also leads to expect little cosmological evolution for the population of bremsstrahlung emitters constituted by groups and clusters. This is because in the X-ray luminosity function $N(L, z)$ the "density evolution" driven at medium-low L by the hierarchical clustering is balanced by the lower luminosities corresponding to a steeper $L - T$ correlation.

In fact, we have investigated and computed elsewhere in detail (Menci & Cavaliere 2000, hereafter MC2000; Cavaliere, Giacconi & Menci 2000, hereafter CGM2000) how the stellar feedbacks (heating combined with ejection) affect the ICM and its X-ray emission $L \propto n^2 R^3 T^{1/2}$, which is particularly sensitive to changes of the central ICM density.

2.4. The SZ probe

In the present paper we stress the *complementary* probe provided by the SZ effect. The CMB modulation $\Delta I/I \approx -2\, y \propto n\, kT\, R$ introduced in §1 provides another observable combination of T and n which depends on the thermal and on the mechanical feedback in a more balanced way.

In parallel with the scaling for L provided by eq. (1), the self-similar scaling for y reads

$$y_{grav} \propto \rho_u^{1/2} T_V^{3/2} \ . \tag{3}$$

We shall investigate how the actual y also *departs* away from y_{grav} due to $n \neq \rho$ and $T \neq T_V$ holding at groups scales, and shall discuss how the relative relative strength y/y_{grav} of the SZ signal is related to entropy. Our investigation will start with computations based upon specific semi-analytic modelling for the baryons in groups and clusters, in particular for those diffuse and hot constituting the ICM.

3. Semi-analytic Modelling of the ICM State and Evolution

In the scenario outlined in §2.3 the processes responsible for the non-gravitational entropy floor in groups in clusters are just the same as those governing the formation history of stars and galaxies. At galactic scales, they tend to suppress the star formation in the earlier and shallower potential wells. The observable consequences include flattening of the local, optical LF function at faint-intermediate luminosities, and a decline of the integrated star formation rate for $z \gtrsim 2$; but the degree of such a decline sensitively depends on the feedback strength in the relevant wells.

The picture has been quantitatively implemented in the so-called semi-analytic models for star and galaxy formation (SAMs, see Kauffmann et al. 1993; Cole et al. 1994; Somerville & Primack 1999). These are built upon the notion of galaxies as baryonic cores located inside DM haloes (White & Rees 1978); they specify – though often in a phenomenological form – how the baryons are cycled among the condensed stellar phase, the cool gas phase and the hot gas phase, under the drive of the merging events that make up the hierarchical evolution of the DM haloes.

Since the very same DM and baryonic processes also play a key role in determining the state of the ICM on scales larger than galactic, we take up the SAM approach in its latest versions, and use it to evaluate the amount of non-gravitational heating of the ICM and to predict the corresponding SZ effect. Our model is necessarly complex as it comprises several processes and many computational steps, so we outline its frame and workings in the form of a flow chart in fig. 1.

3.1. Our SAM: the DM and stellar sectors

We base on an updated version of the SAM originally presented in Poli et al. (1998). In this approach the average over the many possible merging histories of a given structure is performed by convolution over the merging probability functions given by Lacey & Cole (1993) and tested, e.g., by Cohn, Bagla & White (2000); the average also includes the convolution with the probabilities for galaxy aggregations driven by dynamical friction inside common haloes. Toward computing the stellar observables, the model treats the following processes.

1) The DM haloes merge following the hierarchical clustering. The detailed merging histories are important for the problem at hands, since the gas carrying the non-gravitational entropy is pre-heated/expelled from condensations smaller than present-day systems, and is subsequently accreted by larger haloes. The time delays between heating/expulsion and accretion propagate up the structure hierarchy the aftermaths of the feedback.

2) Part of the hot gas mass m_h diffused throughout the haloes cools down in all differently-sized potential wells, then condenses into stars on the timescale τ_*, see Table 1. The amount of cool gas is also controlled by the stellar feedback. This is because the condensation in stars of a mass Δm_* eventually causes stellar winds and SN explosions to release a total non-gravitational energy $E_* = E_{SN}\,\eta_{SN}\,\Delta m_*$ ergs, where $E_{SN} \sim 10^{51}$ erg is the energy of a Type II SN explosion, $\eta_{SN} \approx 3.2\,10^{-3}/M_\odot$ is the efficiency in SNe for the Scalo IMF. Part of such energy is coupled to the gas and reheats an amount of cool gas Δm_h; in the SAMs this is often related to Δm_* by the phenomenological assumption $\Delta m_h = \Delta m_*\,(v/v_h)^{-\alpha_h}$, with typical values for the fraction of reheated gas given by $f_* \equiv \Delta m_h/m_h \sim 10^{-1}$.

The importance of the thermal effects of the feedback is expressed in terms of the above parametrization by the "stellar" temperature

$$kT_* = (1-q_0)\,E_*\,m_p/3\,\Delta m_h\ , \tag{4}$$

where $q_0 \lesssim 10^{-1}$ is the fractional energy going directly into bulk motion of the material; KT_* is to be compared with the virial temperature $k\,T_V$. In the way of a preliminary estimate, note that $kT_* = 0.7\,\Delta m_*/\Delta m_h \gtrsim 0.2$ keV holds for a stellar baryonic fraction exceeding 1/5, the low value actually appropriate only for rich clusters. But $kT_V \approx 0.2$ keV is also the virial temperature corresponding to $M \sim 5\,10^{12}\,M_\odot$; so in galaxies and in poor groups the stellar heating is expected to cause the gas to flow out of the wells. In the numerical model the process is evaluated in detail for all haloes.

In fact, the scale dependence of the feedback is marked by the key parameter α_h. To

identify its relevant range consider the ratio between the work done in moving the gas out of the well and the actual bulk kinetic energy, given by $\epsilon_0 = f_* \, m_h \, v^2 / q_0 \, E_* \propto (v/v_h)^{2-\alpha_h}$. The proportionality constant turns out to be around 0.5 for our fiducial values $E_{SN} = 5\,10^{50}$ erg, $\eta_{SN} = 5\,10^{-3}/M_\odot$ (with the contribution from stellar winds included after Bressan et al. 1994) and for $q_0 = 0.1$; so the reheated gas does escape from the relevant haloes with circular velocities $v \geq v_h$ when one takes $\alpha_h \geq 2$, but it constitutes a fraction f_* that decreases with increasing v.

In the model development presented by MC2000 and CGM2000 we allowed this parameter to range from the extreme value $\alpha_h = 5$ adopted by other workers to our fiducial value $\alpha_h = 2$. The former value (hereafter case $\mathcal{A}$) yields $\epsilon_0 \propto v^{-3}$, which in the shallow early wells constitutes quite a *strong* feedback, well over and above the escape energy barrier; this leads to considerable depletion of the cool baryons and causes the star formation rate to decline sharply for $z \gtrsim 2$. The latter value (hereafter referred to as case $\mathcal{B}$) instead yields a *moderate* and "neutral" feedback corresponding to $\epsilon_0 = \text{const}$; thus even the shallow, galactic haloes are allowed to retain considerable amounts of gas, and the resulting star formation rate is high and rather flat for $z \gtrsim 2$.

The values of this and of other relevant parameters are collected in Table 1. These lead to the B-band luminosity functions of the galaxies and to the cosmic star formation rate presented in MC2000, when the critical universe dominated by Standard Cold Dark Matter is adopted. In the canonical Λ-dominated flat universe the same set of parameters leads to the results presented by Poli et al. (1999) together with the related galaxy sizes and Tully-Fisher relation, and discussed by CGM2000.

3.2. Our SAM: the ICM sector

The SAM used in the present paper includes also the processes relevant to the ICM that have been developed and implemented in MC2000 and CGM2000. In those papers the baryonic component condensed into stars has been used to normalize the model parameters to the optical observations, and the cool gas component has been presented for a final check with relevant data; but our main focus was onto the *hot* gas identified with the ICM, and onto its X-ray emission L. The hot ICM gives also rise to the SZ effect of interest here, so the enumeration begun in §3.1 is continued next, to cover also the following processes relevant to the present scope.

3) The accretion of external gas into the potential wells of groups and clusters sets the boundary condition for the internal gas disposition. To this aim, we compute the density

and temperature of groups and clusters at their virial radius R. This is done in terms of the external temperature T_1 of the gas to be accreted during the merging histories of groups and clusters; T_1 is set not only by the virial equilibrium inside the merging lumps but also by the feedback, and the more strongly so the closer to T_* are the virial values. Our computation comprises the following steps.

First, we assume that the DM density $\rho(r)$ inside the cluster has the form given by Navarro, Frenk & White (1997), and that the density n_1 external to the virial radius R is related to the baryon density Ω_b by $n_1 = \rho(R)\,\Omega_b$.

Next, for a group or cluster of mass M we compute the temperature T_1 of the external infalling gas. In particular, for each lump of mass M' accreted onto M we consider two contributions: the fraction $1 - f_*(M')$ remains inside the potential well of M' at the virial temperature $T_V(M')$, while the fraction $f_*(M')$ is ejected by the winds and the SNe gone off within M', and is heated to the temperature T_* given by eq. (4).

Last, we assume that the external gas is incorporated into the mass M passing through a shock front at a position close to the virial radius R. This is expected because the latter separates the region which is in hydrostatic equilibrium from the outer regions where the motion is dominated by infall (see also Bower et al. 2000), and so defines the transition from infall kinetic to thermal energy of the gas. Shock positions close to R are confirmed by many 1-D and 3-D N-body simulations (e.g., Knight & Ponman 1997; Takizawa & Mineshige 1998; Pantano, Gheller & Moscardini 1998; Governato et al. 2001, in preparation).

Then we compute the density n_2 and the temperature T_2 of the ICM at the boundary R of a group or cluster from the jump conditions at the shock; these are derived from mass and momentum conservation across the shock (the classic Rankine-Hugoniot conditions), and are expressed here in terms of the cluster potential ϕ_2 at the boundary, and of the temperature of the incoming gas. The thermal energy $k\,T_1$ associated with an accreted lump M' is contributed by the virialized component at T'_V and by the ejected component at T'_*, with their weigths $1 - f'_*$ and f'_* introduced above. Thus, the weighted density jump $G \equiv n_2/n_1$ at the shock in the ICM of the considered group/cluster of mass M is given by

$$G(M, M') = f'_*\, g(T'_*) + (1 - f'_*) g(T'_V); \tag{5}$$

the density jump for either component has the form (Cavaliere, Menci & Tozzi 1999) $g(t) = 2\,(1-t) + [4\,(1-t)^2 + t]^{1/2}$ in terms of variable $t = T'_*/T_2$ or $t = T'_V/T_2$, respectively. The full expression for T_2 is given by the same authors (see their eq. 8), but for strong shocks it reads simply

$$k\,T_2(M) \approx \mu m_p \phi_2(M)/3 + 3k\,T_1/2\ , \tag{6}$$

in the approximation of small bulk kinetic energies downstream. Note that for given M' the

weighted jump $G(M)$ increases with M, but saturates to the value 4 when $M \gg M'$, that is, for strong shocks.

For a cluster or group of mass M we obtain the *average* values of the weighted density jump and of the boundary temperature T_2 by integrating over the merging histories; that is, we sum over all accreted lumps M' with their relative merging probabilities by inserting the above expressions eqs. (4) – (6) in the semi-analytic context. This will introduce dispersion in the boundary conditions due to the intrinsic spread of the merging histories; we recall (Cavaliere, Menci & Tozzi 1997, 1999) that the scatter we predicted for the $L-T$ correlation agrees with the findings by Markevitch (1998) and by Allen & Fabian (1998).

We have numerically checked that for weaker and weaker feedback the average of G over the merging histories goes to a constant, so that the self-similar scaling $L \propto T^2$ is recovered as expected.

4) The final process relevant to the ICM is the hydrostatic equilibrium, from which we compute the internal gas density profile, given the above boundary conditions. The gas density run $n(r)/n_2$ is related to the DM density profile $\rho(r)$ in terms of the parameter $\beta = \mu m_H \sigma_2^2/kT_2 \approx T_V/T_2$, the ratio of the DM to the gas specific energy (σ_2 is the 1-D velocity dispersion of the DM at the boundary, related to ϕ_2). While in the case of isothermal ICM and of constant $\sigma(r)$ the run is simply given by $n(r)/n_2 = \rho^\beta(r)/\rho_2^\beta$ (Cavaliere & Fusco Femiano 1976, Jones & Forman 1984), here we use the expressions given by Cavaliere, Menci & Tozzi (1999) for the potential of Navarro et al. (1997) and for a polytropic, but nearly isothermal ICM. [1] Thus, for a mass M at the redshift z we compute the inner ICM profiles $n(x)/n_2$ and $T(x)/T_2$ in terms of the normalized radius $x = r/R$. This is achieved basically with no free parameters (see §5 for a discussion) since the profiles are defined in terms of the boundary conditions and of the depth of the DM potential wells. In particular, for rich clusters $T_2 \gg T_1$ holds and the shocks are strong, so the expression of β obtains simply on using the expression (6) for T_2 to obtain $\beta \approx 1/(1 + 3/2\, T_1/T_V)$. On the other hand, for decreasing M the value of β decreases to attain values $\approx 1/2$ for small groups, which yield gas density profiles significantly shallower than in clusters in agreement with Ponman, Cannon & Navarro (1999).

Fig. 1 provides a representation and a summary of the processes and of the computational steps we use to set the boundary conditions and the internal structure of the ICM. Our assumptions and fiducial choices are discussed in §5.

---

[1] Because $T(x)$ is observed to be close to constant, we distinguish T_V, T_2 and T (the latter may be taken to be the emission-weighted temperature) only when relevant.

We refer to our previous papers MC2000 and CGM2000 for added details and for the results concerning the X-ray observables. In short, these include: β decreases and the relation $L-T$ bends down in moving toward systems of lower T, while $N(L,z)$ shows little or no cosmological evolution, all in good agreement with the observations. In addition, the counts of X-Ray sources from the ICM are predicted to be enhanced corresponding to high values of the star formation rate at $z \gtrsim 1.5$.

Here we epitomize the effectiveness of our model by showing in fig. 2 the central ICM entropy as a function of the X-ray temperature T. Such entropy is given by the ratio $T(r)/n(r)^{2/3}$ and is computed on using the profiles discussed above. Ultimately, these are determined by the global gravitational and by the feedback-induced energies associated with the gas in the infalling clumps.

The result is compared with the data presented by Ponman, Cannon & Navarro (1999) and by Lloyd-Davies, Ponman & Cannon (2000). We recall that entropy is of special value as a state variable for the ICM; in fact, in conditions of long cooling times it keeps the archive - as it were - of the thermal events (different from adiabatic compressions) which are associated with the ICM gravitational heating/compression and with the non-gravitational heating/ejection.

3.3. The SZ effect from our SAM

Here we focus on how we use the above model to compute the SZ effect from the ICM in groups and clusters. The basic relations will be just recalled, having been covered in many excellent reviews beginning with Sunyaev & Zel'dovich (1980) and including Rephaeli (1995) and Birkinshaw (1999).

The Compton parameter induced by the ICM column displaced from the center by the distance w on the plane of the sky may be written as

$$y(w,M) = -2\,\frac{\sigma_T\,k}{m_e\,c^2}\,\int dl\,T(r)\,n(r) = -2\,\frac{\sigma_T}{m_e\,c^2}\,kT_2\,n_2\,R\,\int dx\,\frac{x}{\sqrt{x^2-w^2}}\,\frac{T(x)}{T_2}\,\frac{n(x)}{n_2}\ , \quad (7)$$

where σ_T is the Thompson cross-section, and dl is the path element through the structure along the line of sight. Our SAM provides T_2, n_2 at the boundary and the profiles $T(x)/T_2$, $n(x)/n_2$ all depending on the structure mass M, as described in §3.2. We extend the integrations to infinity, but take into account the temperature and density jumps at $r=R$ across the shock.

The SZ distortion of the CMB spectrum at a frequency ν is given by

$$\Delta I/I = y\, j(\xi)\ . \tag{8}$$

The function $j(\xi)$ depending on $\xi \equiv h\nu/kT_B$ is given by Sunyaev & Zel'dovich (1980) in terms of the temperature T_B of the CMB black-body spectrum; $j \approx -2$ holds in the Rayleigh-Jeans limit $h\nu \ll kT_B$, appropriate for μwave observations. On the other hand, $j(\xi)$ becomes positive beyond $\nu \approx 220$ GHz; so the SZ effect offers a second chance to measure or check y in the sub-mm band, which is clean of radiosources and is now coming of age with the recent or planned sub-mm instrumentation.

The signal from a individual structure at a redshift z in a detector beam with effective aperture θ_b and angular response $\psi(\theta/\theta_b)$ produces the equivalent flux

$$S_\nu = 2\,\frac{(kT_B)^3}{(hc)^2}\,J(\xi)\,2\,\pi\,\int_0^\infty d\theta\,\theta\,\psi(\theta/\theta_b)\,y(\theta) = J(\xi)\,\left[\frac{\overline{y}}{5\,10^{-6}}\right]\left[\frac{\theta_b}{1.5'}\right]^2 \quad \mathrm{mJy}. \tag{9}$$

Here the function $J(\xi)$ is related to $j(\xi)$ as described by Sunyaev & Zel'dovich (1980); angles θ correspond to w as given by $\theta = w/D_A$, D_A being the angular diameter distance; the area averaged Compton parameter is given by $\overline{y} = 2\,\pi\,\int_0^\infty\, d\theta\,\theta\psi(\theta/\theta_b)\,y(\theta)/\pi\theta_b^2$. For an individual structure the interesting condition occurs when it fills the aperture, that is, when $\theta_b \lesssim R/D_A$.

A related observable is provided by the cosmic average of the Compton parameter, that is, the integrated distortion of the CMB spectrum produced by all groups and clusters distributed in a given beam along the line of sight out to the redshift z. This is given by

$$\langle y\rangle = \int_0^z dz'\,\frac{dV(z')}{dz'}\,\int dM\ N(M,z')\left(\frac{R}{D_A}\right)^2\,\int_0^\infty d\theta\,\theta\,\psi(\theta/\theta_b)\,y(M,\theta)\ , \tag{10}$$

where $V(z)$ is the cosmological volume, and we take the mass function $N(M,z)$ to have the Press & Schechter form that lies at the base of the all SAM descriptions of DM merging process.

Finally, the source counts corresponding to fluxes larger than S_ν (Korolëv, Sunyaev & Yakubtsev 1986) are given by

$$N(>S_\nu) = \int_0^\infty dz\,\frac{dV(z)}{dz}\,\int_{\overline{M}(S_\nu,z)}^\infty dM\,N(M,z)\ , \tag{11}$$

where $\overline{M}(S_\nu,z)$ is the mass of a cluster (or group) that at the redshift z produces the flux S_ν, computed after eqs. (8) and (9).

4. Results

We plot in figs. 3 and 4 the relation $y - T$ that relates the Compton parameter y for individual groups or clusters to their ICM temperature. The values provided by the self-similar scaling are shown by dotted lines, while dashed and solid lines represent what we predict for moderate (case $\mathcal{B}$) and strong (case $\mathcal{A}$) feedback, respectively.

Fig. 3 refers to the critical universe with $h = 0.5$, $\Omega_b = 0.06$ and with DM perturbation amplitude $\sigma_8 = 0.67$ (SCDM cosmology/cosmogony hereafter). Fig. 4 refers to a flat universe with $\Omega_\Lambda = 0.7, \Omega_0 = 0.3$, $h = 0.7$, $\Omega_b = 0.04$ and $\sigma_8 = 1$ (in the following, ΛCDM cosmology/cosmogony). In both figures the bottom panel shows the $y - T$ relation with y normalized to the self-similar scaling $y_{grav} \propto T^{3/2}\rho^{1/2}$. The latter would yield a horizontal line in this plot, so that departures from this behaviour mark the effects of non-gravitational processes; it is seen that the stronger is the feedback at group scales, the larger is the departure .

As to observability, note from figs. 3, 4 and from eqs. (9), (10) that the difference $\Delta y = y - y_{grav}$ expected at the scale of galaxy groups ($T \sim 1$ keV) is of order $5\,10^{-6}$ or smaller, corresponding to $\Delta T/T \lesssim 25\,\mu$K. Observing such values constitutes a challenging proposition, but one becoming feasible for groups and poor clusters with size $R \sim 0.5 \div 0.7\,h^{-1}$ Mpc at $z \sim 5\,10^{-2}$ (and containing only weak radiosources), in the following instrumental conditions: last generation radiotelescopes (see Komatsu et al. 2000), with low internal noise and beams of a few arcminutes, using long integrations (the subtraction of atmospheric noise is favoured by the narrow throws required for these objects); in the near future, arrays like AMiBA (see Lo, Chiueh, & Martin 2000); in perspective, many superposed orbits of the planned *PLANCK* Surveyor mission within its apertures of $5' \div 10'$ (see De Zotti et al. 2000), and ALMA with its μ K sensitivity over angular scales from a few to tens of arcseconds (see www.ALMA.nrao.edu).

The detection of y in groups may be disturbed by surrounding large scale structures aligned along the line of sight. However, the probability for this to occur is low, since such structures compared with virialized condensations have lower temperatures and densities lower by factors ~ 30 at least; only when their extension along the line of sight exceeds the size of a galaxy group by factors larger than 30 a comparable SZ signal will be produced. We add that the scatter we find in the $y - T$ relation is smaller than $\Delta y/y = 0.15$ for all temperatures; so even in our moderate feedback case $\mathcal{B}$ the predicted *trend* of $y - T$ departs neatly from y_{grav} below a few keVs, and even upper bounds to y may be of value.

In fig. 5 we plot (for both the SCDM and the ΛCDM cosmology/cosmogony) the predicted SZ source counts, and in fig. 6 we show also the contribution to the cosmic

Compton parameter from all virialized structures distributed along the line of sight. Note that the difference bewteen the two feedback cases $\mathcal{A}$ and $\mathcal{B}$ (solid lines and dashed lines, respectively) is small for such integrated observables (the curves corresponding to the self-similar case would closely overlap those relative to the moderate feedback case $\mathcal{B}$). This is because small and/or distant structures not filling a telescope beam contribute to these two observables with weights given by the system radius squared (see eq. 10-11); this circumstance underplays the contribution of the groups, the structures most sensitive to feedback effects. On the other hand (see Cavaliere, Menci & Setti 1991; Bartlett & Silk 1994), this very feature makes $N(> S_\nu)$ suitable as a cosmogonical probe, since the contributions of the cosmogonical parameters like the amplitude σ_8 of the spectrum of the initial DM perturbations override those from the state and evolution of the ICM.

Similar results concerning $\langle y \rangle$ from the virialized structures have been found by Valageas & Silk (1999) (see also Valageas & Schaeffer 2000). These authors add the contributions produced by the gas inside lower density structures and by truly intergalactic gas , which they find to depend sensitively on the heating model; this is not unexpected from non-virialized gas that fills bigger volumes and can absorb larger energies.

5. Discussion

Here we focus the basic features shared by a number of current models of the ICM (MC2000, CGM2000; Wu, Fabian & Nulsen 1998; Valageas & Silk 1999; Bower et al. 2000), in order to discuss to what extent our predictions concerning the SZ effect are robust. We first stress the basic blocks shared by such models. Next we discuss our specific treatement of the boundary conditions in terms of shock jumps. Then we discuss why the shocks are effective in amplifying the impact of non-gravitational energy injections. Finally, we show how the departure of the $y - T$ relation from its gravitational counterpart is related to the corresponding departure of the $L - T$ relation; the model-independent link is constituted by the entropy discharged by the injection of non-gravitational energy, but the actual size of such departures depends on the feedback strength.

5.1. Basic blocks

a) Part of the baryons are subtracted out of the hot phase by cooling and are locked in the stars formed, to be only in part recycled by stellar winds.

This actually constitutes a minor negative contribution to the mass of the hot phase.

b) The energy fed back by the condensing baryons, either to fuel black holes at the galactic centers or to form massive stars followed by winds and SNe, heats up a fraction of the intergalactic medium. In our model the energy injection is $E_* \approx 3\,10^{48}$ erg per solar mass of stars formed, the fraction is $f_* \lesssim 0.15$ and the stellar heating temperatures are $kT_* \sim 0.2$ keV; the net outcome is to produce in groups a central density $n \sim 10^{-4}$ cm^{-3}, lower than in clusters. Since such gas is recovered by larger haloes during later merging events (with the delays described in §3.1), the effects propagate a number of steps up the mass hierarchy, so that the $L - T$ relation departs away from $L_{grav} \propto T_V^2$ at temperature considerably higher than 0.5 keV. A corresponding feature is also present, e.g., in the elaborate model used by Bower et al. (2000); in their model, as well as in ours, the gas fraction inside the virial radius is lower in groups than in clusters.

c) Equilibrium is re-established soon after minor and intermediate merging events, that is, over sound crossing times which are somewhat shorter than the structures' dynamical times. In such conditions, the pressure gradient balances gravity and a β-model holds.

d) Once equilibrium is assumed, a key role is played by the boundary conditions that set normalization and shape (specifically, the values of β) of the ICM density profiles. In particular, the pressure balance at the boundary $r \approx R$ clearly constitutes the key condition; we add that such a balance is to include the ram pressure due to the bulk motion v_1 of the infalling gas out of equilibrium, to read $p_2 \approx p_1 + n_1 m_H v_1^2$ in conditions with low bulk kinetic energy downstream.

e) Since the ICM state is observed to be close to isothermal (T may decrease out to R hardly by a factor 2, see Nevalainen, Markevitch, & Forman 2000) a sharp boundary – that is, some sharp drop or discontinuity of T and/or n – is to take place at $r \approx R$, lest the thermal exceeds the integrated gravitational energy.

Model-dependent features, which however affect to a lesser extent the profiles of the ICM in virialized structure, include: the exact value of the polytropic index (close to 1 anyway) and the detailed form of the underlying DM potential (see the discussion by Cavaliere, Menci & Tozzi 1999); the parameters other than the feedback exponent α_h that are introduced in the various SAMs only to tune the optical luminosity function and the Tully-Fisher relation for the galaxies (cf. Cole et al. 1994 with Cole et al. 2000).

5.2. Large-scale shocks

It is also widely agreed that shocks provide an effective coupling of the gravitational to the thermal energy in the ICM.

In our picture, we take up from the results of the simulations referred to in §3.2 the notion that *external* accretion shocks do establish a discontinuity at about $r \approx R$, with low bulk velocities left downstream; observational evidence of large scale shocks related to violent merging events is reported by Roettiger, Stone & Mushotzky (1998); Roettiger, Burns & Stone (1999); Markevitch, Sarazin & Vikhlinin (1999). Across such shocks the above stress conservation combined with with mass conservation yields the classic Rankine-Hugoniot jump conditions for T and n. Without further ado these produce a non-linear increase of $G \equiv n_2/n_1$ from 1 to 4 as the infall flows become increasingly supersonic, that is, as T_V/T_1 increases.

Note that the merging events that yield the largest contributions to $G(T_2/T_1)$ are the numerous ones (more than 90%) with minor partners having mass ratios smaller than 1/4, which may be appropriately described as constituting an "accretion" inflow of the DM component as well as of the baryonic component (see Raig, Gonzalez-Casado & Salvador-Sole 1998). Such minor events contribute the majority of the mass increase (more than 50%), and imply lower temperatures $kT_1 \lesssim 1$ keV (whether of gravitational or of stellar origin) for the external gas they involve, leading to more supersonic gas inflows. The summed action of these events is as close to isotropic as permitted by the surrounding large scale structure (see Tormen 1997; Colberg et al. 1999); re-establishing the equilibrium then is more like a continuous re-adjustement to the accretion inflow.

On the other hand, given the external conditions the gas inflow is bound to be more supersonic on average when it takes place into the deeper wells provided by the richer clusters where $v_1 \gtrsim 1000$ km s^{-1} is attained; this leads to expect larger entropy depositions in the outer regions of rich clusters, as in fact observed (Lloyd-Davies, Ponman & Cannon 1999). In poor groups, instead, where the stellar heating temperatures match the virial ones to give $kT_* \sim 0.3 - 0.5$ keV, the shocks degenerate into sonic, adiabatic transitions; here all internal densities scale down proportionally to $n_2 \to n_1$, so $L \propto n_2^2$ is bound to plunge down toward $L \propto n_1^2 \propto n_2^2/16$.

To see how the departures from the self-similar scalings begin and end, one can make use of two opposite approximations, rather crude but simple: when the pre-shock temperature T_1 is low, the strong shock approximation yields $kT_2 \approx kT_V + 3\,kT_1/\,2$, see eq. (6); on the other hand, the lower bound to all temperatures is constituted by T_*. For decreasing depths of the wells these approximations show that the decline of $\beta \propto T_V/(T_V + 3T_1/2)$ begins slowly, then becomes faster like $\beta \propto T_V/T_*$ in shallow wells; this implies correspondingly flatter density profiles. Similarly but more strongly, $L \propto n_1^2\, g^2(T/T_1) \approx 16 n_1^2\,(1 - 15\,T_1/8\,T_2)$ departs from $L_{grav} \propto 16\,n_1^2$ slowly at first in deep wells, but eventually plunges toward $L \propto n_1^2$ in shallow wells.

A final remark concerns the normalization of the Compton parameter y related to the shock condition. In our model, the boundary values for the density and the temperature are fixed by the shock jumps in terms of the external density n_1 and of the gravitational potential ϕ_2 at $r = R$ (see eq. 7). Now, $n_1 \propto \Omega_b$ holds, while ϕ_2 depends both on the shape of the gravitational potential and on the location of the boundary at $r \approx R$. For our fiducial choice of $\Omega_b = 0.04$ and of the Navarro et al. (1995) potential, our shock or boundary location (supported by the N-body simulations referred to in §3.2) leads to a normalization of the y parameter in agreement with the observed values; for example, for a Coma-like cluster with $T_V \approx 8$ keV, we obtain $y \approx 10^{-4}$, closely independent of the feedback, see fig. 4; this is in good agreement with the measured value, see Herbig et al. (1995). The same normalization can be obtained on changing the value of Ω_b in the range $0.02 - 0.06$ allowed by the canonical primordial nucleosynthesis, and on retaining the same DM potential but readjusting the shock position within the range $0.85 - 1.15\ R$ compatible with the N-body simulations.

5.3. Amplification and feedback

It is intrinsic to the present model that the departures from the gravitational scaling are non-linearly *amplified*, due to the varying shock strengths set by the depth kT_V of the potential wells compared with kT_*. For a given departure, such an amplification *lowers* the requirements for the non-gravitational energy injection. Indeed, the excess central entropy $e^S \propto kT/n^{2/3}$ observed in groups over the self-similar expectations (see fig. 2) can be obtained with a moderate energy injection E_* leading to $T \approx T_V + T_*$ with $k\,T_* \approx 0.3$ keV, provided the central density at the group scale is decreased relative to clusters by a factor around 10. In our model such a decrement results in part from the boundary density jump (lower than in clusters by a factor 4), and in part from the shallow gas density profile due to the lower values of β (about half than in clusters).

Thus, the presence of shock amplification allows us to consider *conservative* quantities for the feedback, namely, energy contributed by stellar winds plus by SN explosions adding up to $E_* = \eta_{SN}\, 5\, 10^{50} \approx 3\, 10^{48}$ erg per $M_\odot$ of stars formed. Note also that the two contributions are largely separated and undergo different amounts of cooling, lesser (if anything) for the winds.

Stellar winds and amplification go a couple of steps toward meeting the concerns about prompt radiative cooling of the SN outputs which may limit the fraction available for action at galactic or group scales. As is well known, the issue is a thorny and debated one. On the one hand stands the intrinsic sensitivity of the cooling to density clumpiness (see, e.g.,

Thornton et al. 1998). On the other hand, momentum and thermal energy are carried outward of the sites of star formation in the form of blast waves and shocks, in fact as SN Remnants. It is widely agreed (see Ostriker & McKee 1988) that these may easily overlap before they enter a strong radiative phase, especially when they are driven by type II SNe produced by correlated massive star formation, and when they are helped by the tunnel network in the ISM. So they merge their hot and thin interiors, break out of the galaxies in the form of superbubbles, and discharge their high entropy content into the galaxian outskirts; this is then mixed throughout the ICM.

Additional sources of non-gravitational heating may be provided by Active Galactic Nuclei shining at the center of developing galaxies (see Wu, Fabian & Nulsen 1999; Valageas & Silk 1999; Aghanim, Balland & Silk 2000). The AGNs are fed at sub-pc scales by accreting black holes; their outputs are huge, but the effective coupling within galaxies or groups of such energy to the ICM within galaxies or groups is even more uncertain than for the SNe. Such coupling would require quite some tuning to yield just the observed $L-T$ correlation (P. Madau, private communication); the intrinsic instability of the cooling may easily drown any correlation into a large intrinsic scatter. Treating such processes in full is beyond the scope of the present paper and will be undertaken elsewhere.

5.4. SZ effect vs. X-ray emission

As can be noted from figs. 3 and 4, the departure from self-similarity we find from our model in the $y-T$ relation for groups and clusters features an *inverse* y-dependence on the strength of the feedback, which sets in below $T\sim 1$ keV. This behaviour is similar to that of the $L-T$ relation for groups and clusters of galaxies.

The correspondence is explained by the model-independent relation which follows from combining the definitions of S and of the Compton parameter y with its self-similar scaling given by by eq. (3), to read

$$e^{S-S_{grav}}=(y/y_{grav})^{-2/3}\,(T/T_V)^{5/3}\ . \tag{12}$$

We recall from §5 that T exceeds T_V due to the non-gravitational heating, and the excess becomes more and more relevant in moving from rich clusters to poor groups. The above eq. shows than that an internal heating source rising the entropy content will result in lower values of y compared to the self-similar expectations at the scale of groups.

The counterpart of eq. (12) for the X-ray emission reads

$$e^{S-S_{grav}}=(L/L_{grav})^{-1/3}\,(T/T_V)^{7/6}\ , \tag{13}$$

again model-independently. Assuming the two observables are associated (albeit with different shape factors) with ICM confined within comparable sizes, the two equations combine to yield

$$y/y_{grav} = (L/L_{grav})^{1/2}\,(T/T_V)^{3/4}\ . \tag{14}$$

The above equations highlight in a *model-independent* way the inverse nature of both the $S-y$ and the $S-L$ relations. So the entropy excess observed in groups of galaxies implies a related deficit of *both* the X-ray luminosity as indeed is found in the observed $L-T$ correlation, and of the SZ effect as here predicted. In both cases the dependence on the temperature is instead direct, and actually stronger in the $S-y$ relation.

The point to emphasize is that these two probes are *independent* observationally; in fact, they are measured in such distant bands as X-rays and microwaves, with very different instrumentations subject to different systematics. In addition, the SZ effect can be measured also at sub-mm wavelengths, which provide a positive $\Delta I/I$ with systematics different yet. Finally, the selections are intrisically different in the μw/sub-mm and in the X-ray bands, with the SZ signal being much *less* sensitive than the X-ray emission to internal density clumpiness or enhancements. Thus, while either observable may be subject to its own observational biases, background subtraction or scatter (see Mahdavi et al. 1997; Roussel, Sadat & Blanchard 2000), the *combined* evidence will be highly significant and strongly constraining for the non-gravitational heating mechanisms.

6. Conclusions

In this paper we have computed and presented three observables related to the SZ effect from the ICM in groups and clusters of galaxies, namely, the $y-T$ correlation, the source counts and the contribution to the cosmic SZ effect. We based our computations on the specific semi-analytic model (SAM) described in §3; this is built upon the hierachical merging histories of the DM component of such structures, and provides stellar and X-ray observables in agreement with the data. The picture underlying our SAM is widely shared, and its main blocks are common (as discussed in §5) to other SAMs also aimed at explaining the optical and X-ray observations.

One key feature is the energy and momentum fed back into the ICM by the condensing baryons. This has the effect of pre-heating the baryons that fall into groups and clusters during their merging history. The shock front forming between the infalling and the internal gas amplifies the effect of the non-gravitational heating on the density distribution of the gas in a way which depends on the cluster or group temperature T. The net effect is to

break the (approximate) scale-invariance of the DM quantities in *virialized* structures, particulary in galaxy groups with $kT \lesssim 1$ keV compared to rich clusters. The effect of such processes on the X-ray properties of groups and clusters has been investigated in our previous papers; here we have shown that the SZ effect constitutes a *complementary* probe of the non-gravitational heating of ICM. In particular we emphasize the following results.

• The measure of the Compton parameter y from deep, targeted observations of groups and clusters and the resulting $y - T$ correlation provide a direct probe of the energy discharged into the ICM and archived there in conditions of long cooling times. Specifically, for energy injections dumped into the ICM within galaxies or groups we predict the $y - T$ correlation to bend down systematically relative to the self-similar expectations (see §4, figs. 3-4). In §5 we discuss the generic aspects of the *trend*: larger injection - smaller y at group scales, that we expect from any reasonably complete model. The level of such departures will be similar to ours for feedback models able to reproduce the bent shape of the $L - T$ relation in X-rays. This conclusion is substantiated by eqs. (12)-(14) which show *model-independently* that heating sources rising the internal entropy in groups to the observed "floor" will result in observably low values of y compared to the self-similar expectations.

• The integrated SZ effects from structures (i.e., the counts $N(> S_\nu)$ of SZ sources associated with virialized structures and their contribution $\langle y \rangle$ to cosmic SZ effect (see figs. 5-6) are dominated by clusters less affected by the feedback, even less by its details.

To conclude, the emerging picture is one where the close scale-invariance of the *gravitational* energy released over large scales under the drive of the DM dynamics is broken by the *nuclear* energy that at small scales drives the stellar life and death; the break-even point should occur at the transitional mass scale $M \sim 10^{13} M_\odot$ where $kT_V \approx kT_* \approx 0.3$ keV holds. The specific way in which baryons break the DM scale-invariance can be probed with several *complementary* but observationally *independent* observables which include: the bent X-ray luminosity-temperature correlation; the weak or absent evolution of the X-ray luminosity functions; excess counts of the ICM X-ray sources correlated with high rates of cosmic star formation at $z \gtrsim 1.5$; the shape and evolution of the optical luminosity function of the galaxies; finally, the SZ effect as proposed here, and in particular the bent $y - T$ relation from clusters to groups.

Acknowledgements. This work benefited at all stages from helpful exchanges with G. De Zotti. We are grateful to F. Melchiorri for discussions of his observational strategies with MITO, to A. Lapi for critical reading, and to our referee for constructive and helpful comments. Partial grants from ASI and MURST are acknowledged.

REFERENCES

Aghanim, N., Balland, C., Silk, J. 2000, A&A, 357, 1

Allen, S.M, & Fabian, A.C. 1998, MNRAS, 297, L56

Bartlett, J.G., & Silk, J. 1994, ApJ, 423, 12

Baugh, C.M., Cole, S., Frenk, C.S., & C.G. Lacey 1998, ApJ, 498, 504

Birkinshaw, M. 1999, in *3K Cosmology*, L. Maiani, F. Melchiorri & N. Vittorio eds. (Woodbury: American Institute of Physics) 476, p. 298

Bower, R.G. 1997, MNRAS, 288, 355

Bower, R.G., Benson, A.J., Baugh, C.M., Cole, S., Frenk, C.S., & Lacey C.G. 2000, preprint [astro-ph/0006109]

Bressan, A, Chiosi, C, & Fagotto, F. 1994, ApJ SS, 94, 63

Carlstrom, J.E. et al. 2000, Phys. Scripta, T 85, 148-155

Cavaliere, A., Menci, N., & Setti, G. 1991, A&A, 245, 21

Cavaliere, A., Menci, N., & Tozzi, P. 1997, ApJ, 484, L21

——————————————— 1999, MNRAS, 308, 599

Cavaliere, A., Giacconi, R., & Menci, N. 2000, ApJ, 528, L77 (CGM2000)

Cohn, J.D., Bagla, J.S., & White, M. 2000, preprint [astro-ph/0009381]

Colberg, J.M., White, S.D.M., Jenkins, A., & Pearce, F.R., 1999, MNRAS, 308, 593

Cole, S., Aragon-Salamanca, A., Frenk, C.S., Navarro, J.F., & Zepf, S.E. 1994, MNRAS, 271, 781

Cole, S., Lacey, C., Baugh, C., Frenk, C.S., & 2000, MNRAS, in press [astro-ph/0007281]

De Zotti, G. et al. 2000, in *3K Cosmology*, L. Maiani, F. Melchiorri & N. Vittorio eds. (Woodbury: American Institute of Physics) 476, p. 204

Fujita, Y., & Takahara, F. 2000, ApJ, 536, 523

Fukugita, M., Hogan, C.J., & Peebles, P.J.E. 1997, preprint [astro-ph/9712020]

Gheller, M., Pantano, O. & Moscardini, L. 1998, MNRAS, 296, 85

Helsdon, S.F., & Ponman, T.J 2000, MNRAS, in press [astro-ph/0002051]

Jones, C., & Forman, W. 1984, ApJ, 276, 38

Kaiser, N. 1986, MNRAS, 222, 323

Kaiser, N. 1991, ApJ, 383, 104

Kauffmann, G., White, S.D.M., & Guiderdoni, B. 1993, MNRAS, 264, 201

Knight, P.A., Ponman, T.J. 1997, MNRAS, 289, 955

Komatsu, E. et al. 2000, PASJ, 53, 57

Korolëv, V.A., Sunyaev, R.A., & Yakubtsev, L.A. 1986, PAZh, 12, 141

Herbig, T., Lawrence, C.R., Redhead, A.C.S., Gulkis, S., 1995, ApJ, 110, L5

Lacey, C., & Cole, S. 1993, MNRAS, 262, 627

Lloyd-Davies, E.J., Ponman, T.J., & Cannon, D.B 2000, MNRAS, 315, 689

Lo, K.Y., Chieu, T., Martin, R.N., 2000, AAS, 197, 560

Mahdavi, A., Boehringer, H., Geller, M.J., Ramella, M., 1997, ApJ, 483, 68

Markevitch, M. 1998, ApJ, 504, 27

Markevitch, M., Sarazin, C.L., & Vikhlinin, A. 1999, ApJ, 521, 526

Menci, N., & Cavaliere, A. 2000, MNRAS, 311, 50 (MC2000)

Navarro, J.F., Frenk, C.S., & White, S.D.M. 1997, ApJ, 490, 493

Nevalainen, J., Markevitch, M., & Forman, W. 2000, in *Large Scale Structure in the X-ray Universe*, Plionis, M. & Georgantopoulos, I. eds. (Atlantisciences: Paris, France), p.393

Ostriker, J.P., & McKee, C.F. 1988, Rev. Mod. Phys. 60, n. 1

Peebles, P.J.E. 1993, *Principles of Physical Cosmology* (Princeton: Princeton Univ. Press)

Ponman, T.J., Cannon, D.B., & Navarro, J.F. 1999, Nature, 397, 135

Poli, F., Giallongo, E., Menci, N., D'Odorico, S., & Fontana, A. 1999, ApJ, 527, 662

Raig, A., Gonzalez-Casado, G., & Salvador-Sole, E. 1998, ApJ, 508, L129

Rephaeli, Y. 1995, ARAA, 33, 541

Roettiger, K., Burns, J.O. Stone, J.M. 1999, ApJ, 518, 603

Roettiger, K., Stone, J.M, & Mushotzky, R.F 1998, ApJ, 493, 62

Rosati, P., Della Ceca, R., Norman, C., & Giacconi, R. 1998, ApJ, 492, 21

Roussel, H., Sadat, R., & Blanchard, A., 2000, A&A, 361, 429

Saunders, R.D.E., & Jones, M.E. 2000, to appear in Proc. IAU Symposium 201

Somerville, R.S., & Primack, J.R. 1999, MNRAS, 310, 1087

Sunyaev, R.A., & Zel'dovich, Ya.B. 1972, Comm. Astroph. Sp. Sc., 4, 173

Sunyaev, R.A., & Zel'dovich, Ya.B. 1980, ARA&A 18, 537

Takizawa, M., & Mineshige, S. 1998, ApJ, 499, 82

Tormen, G., 1997, MNRAS, 290, 411

Tozzi, P. & Norman, C. 2000, preprint [astro-ph0003289]

Thornton, K., Gaudlitz, M., Janka, H.Th., & Steinmetz, M. 1998, ApJ, 500, 95

Valageas, P., & Silk, S. 1999, A&A, 1999, 350, 725

Valageas, P., & Schaeffer, R., 2000, A&A, 359, 821

White, S.D.M., & Fabian, A.C. 1995, MNRAS, 273, 72

White, S.D.M., Navarro, J.F., Frenk, C.S., & Evrard, A.E. 1993, Nature, 366, 429

White, S.D.M., & Rees, M.J. 1978, MNRAS, 183, 341

Wu, K.K.S., Fabian, A.C., Nulsen, P.E.J. 1998, MNRAS, 301, L20

Wu, K.K.S., Fabian, A.C., Nulsen, P.E.J. 1999, preprint [astro-ph/9907112]

FIGURE CAPTIONS

Fig. 1. We show in the form of a flow chart diagram the processes we consider and the computational steps we use to compute in the DM haloes the ICM profile and its boundary conditions.

Fig. 2. As a preliminary test of our SAM model, we show the predicted central entropy of the ICM as a function of the temperature for the strong feedback case $\mathcal{A}$ (solid line) and the moderate feedback case $\mathcal{B}$ (dashed line), compared with the data from Ponman, Cannon & Navarro (1999). We also show as a dotted line the result from the self-similar scaling, eq. (2). All lines refer to the SCDM cosmogony/cosmology with $\Omega = 1$, $\Lambda = 0$, $h = 0.5$, $\Omega_b = 0.06$, and $\sigma_8 = 0.67$. The ΛCDM case yields similar results.

Fig. 3. The top panel shows the relation we predict between the (area averaged) Compton parameter y for individual groups and clusters and the temperature; the solid line refers to the strong feedback case $\mathcal{A}$, the dashed line to the moderate feedback case $\mathcal{B}$, while the self-similar scaling is plotted as a dotted line. SCDM cosmology/cosmogony. The bottom panel shows the same correlation but with the Compton parameter normalized to its self-similar scaling given by eq. (3)

Fig. 4. Same as fig. 2 but for the ΛCDM cosmogony/cosmology.

Fig. 5. The predicted source counts as a function of the SZ flux at 100 GHz, see eqs. (10) and (11). Solid and dashed lines refer to the feedback cases $\mathcal{A}$ and $\mathcal{B}$, respectively. The curve relative to the self-similar case would overlap that referring to case $\mathcal{B}$. The bottom line is computed for the SCDM cosmogony/cosmology, while the one on top refers to the ΛCDM case.

Fig. 6. The contribution to the cosmic Compton parameter (see eq. 11) from the ICM inside *virialized* structures, groups and clusters of galaxies, distributed out to the redshift z; SCDM (bottom lines), and ΛCDM universe (top lines) are considered. The solid and dashed lines refer to the feedback strengths $\mathcal{A}$ and $\mathcal{B}$, respectively.

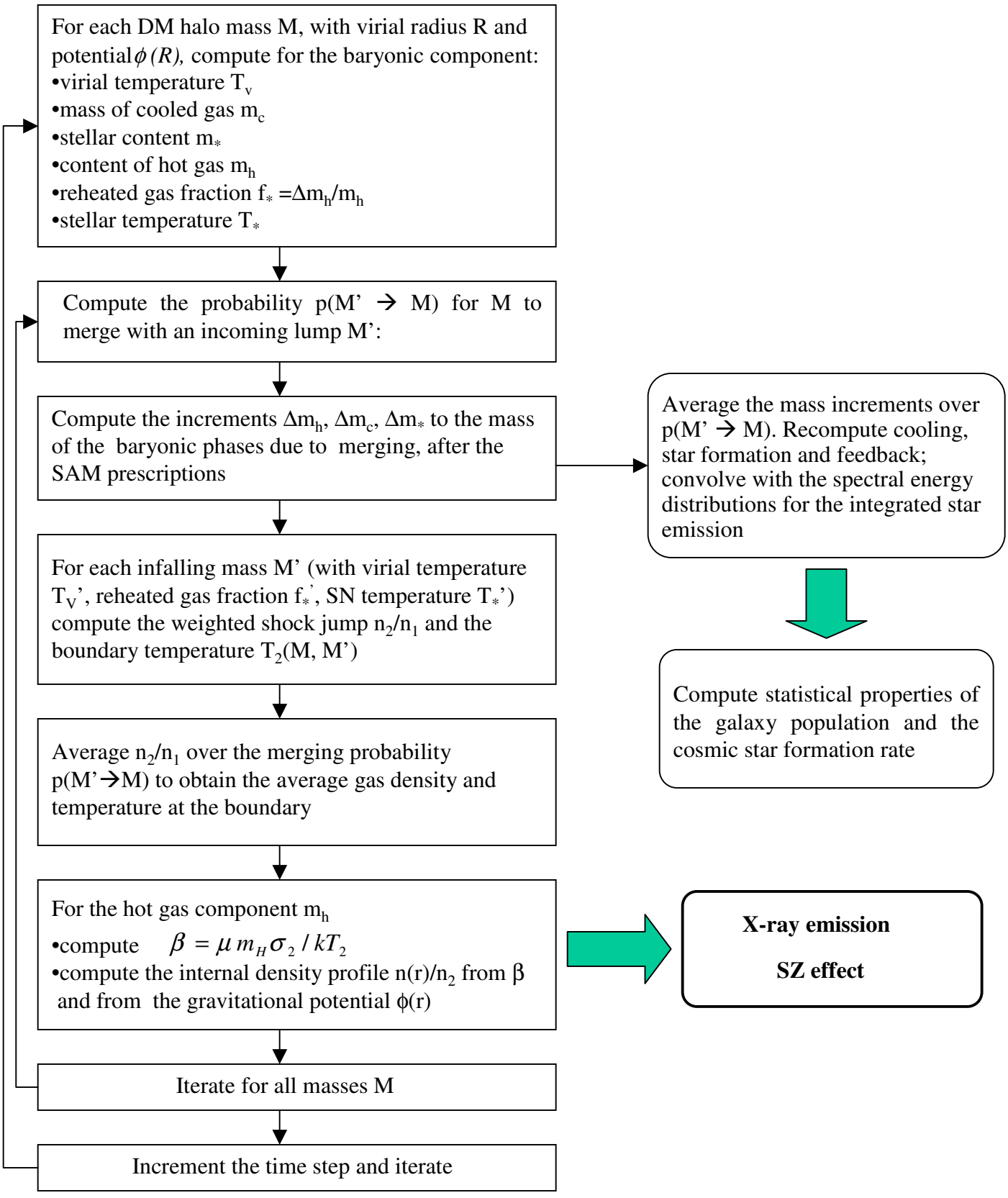
For each DM halo mass M, with virial radius R and potential $\phi(R)$, compute for the baryonic component:
•virial temperature T_v
•mass of cooled gas m_c
•stellar content m_*
•content of hot gas m_h
•reheated gas fraction $f_* = \Delta m_h / m_h$
•stellar temperature T_*
Compute the probability p(M' → M) for M to merge with an incoming lump M':
Compute the increments Δm_h, Δm_c, Δm_* to the mass of the baryonic phases due to merging, after the SAM prescriptions
Average the mass increments over p(M' → M). Recompute cooling, star formation and feedback; convolve with the spectral energy distributions for the integrated star emission
Compute statistical properties of the galaxy population and the cosmic star formation rate
For each infalling mass M' (with virial temperature T_V', reheated gas fraction f_*', SN temperature T_*') compute the weighted shock jump n_2/n_1 and the boundary temperature $T_2(M, M')$
Average n_2/n_1 over the merging probability p(M'→M) to obtain the average gas density and temperature at the boundary
For the hot gas component m_h
•compute $\beta = \mu m_H \sigma_2 / kT_2$
•compute the internal density profile $n(r)/n_2$ from β and from the gravitational potential φ(r)
X-ray emission
SZ effect
Iterate for all masses M
Increment the time step and iterate

Fig. 1

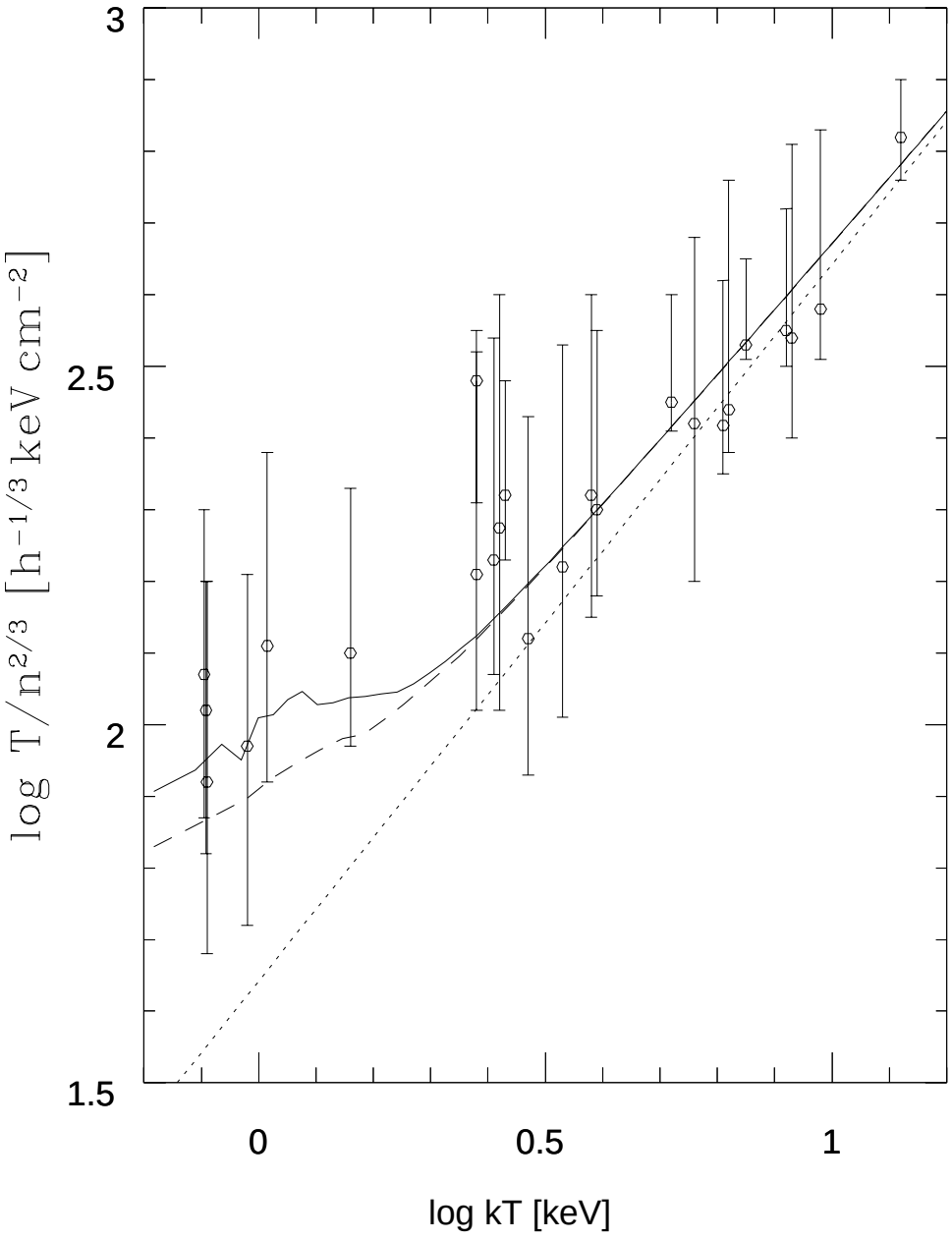

Fig. 2

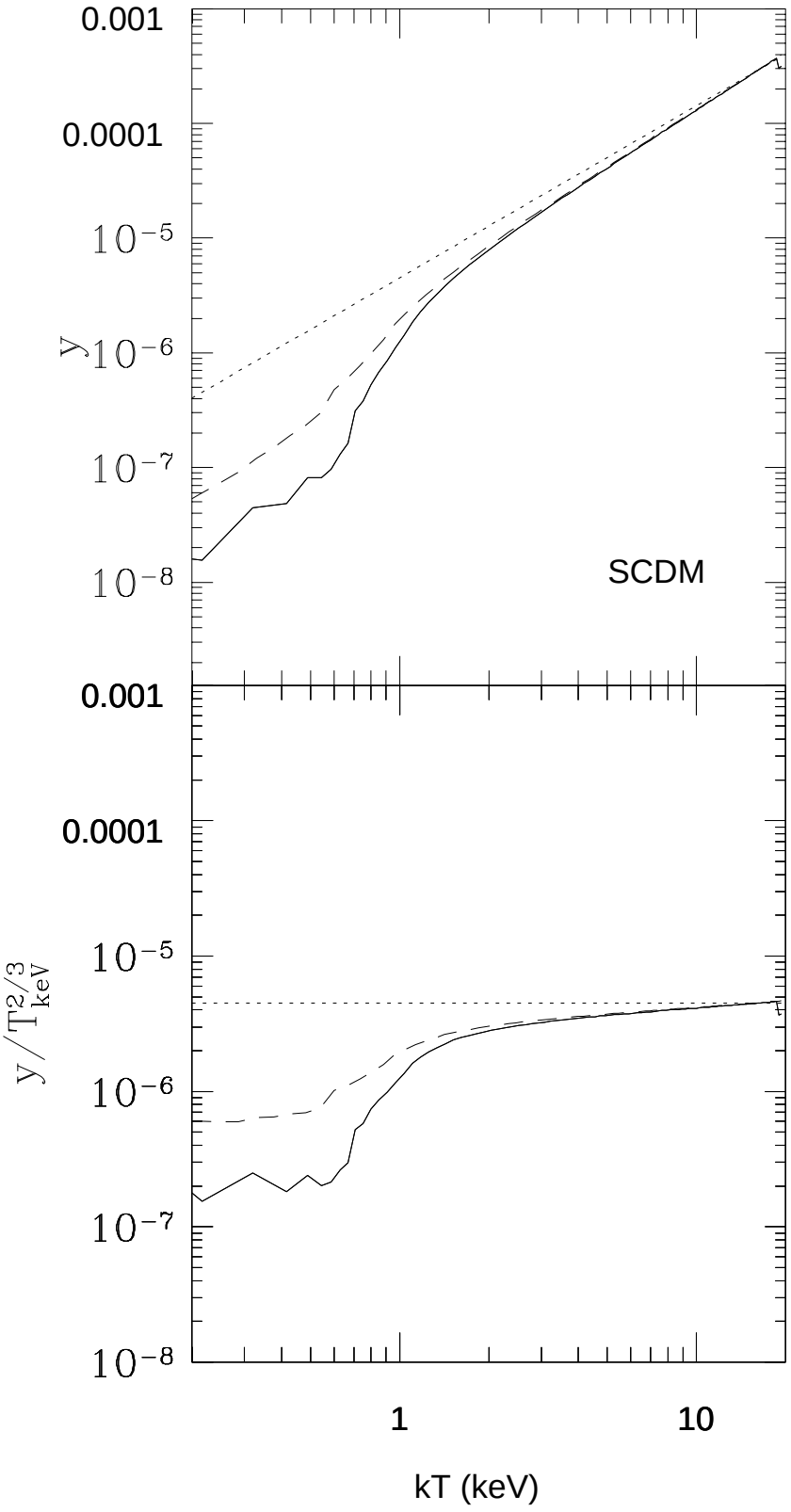
0.001
0.0001
10^{-5}
10^{-6}
10^{-7}
10^{-8}
y
SCDM
0.001
0.0001
10^{-5}
10^{-6}
10^{-7}
10^{-8}
$y/T_{keV}^{2/3}$
1
10
kT (keV)

Fig. 3

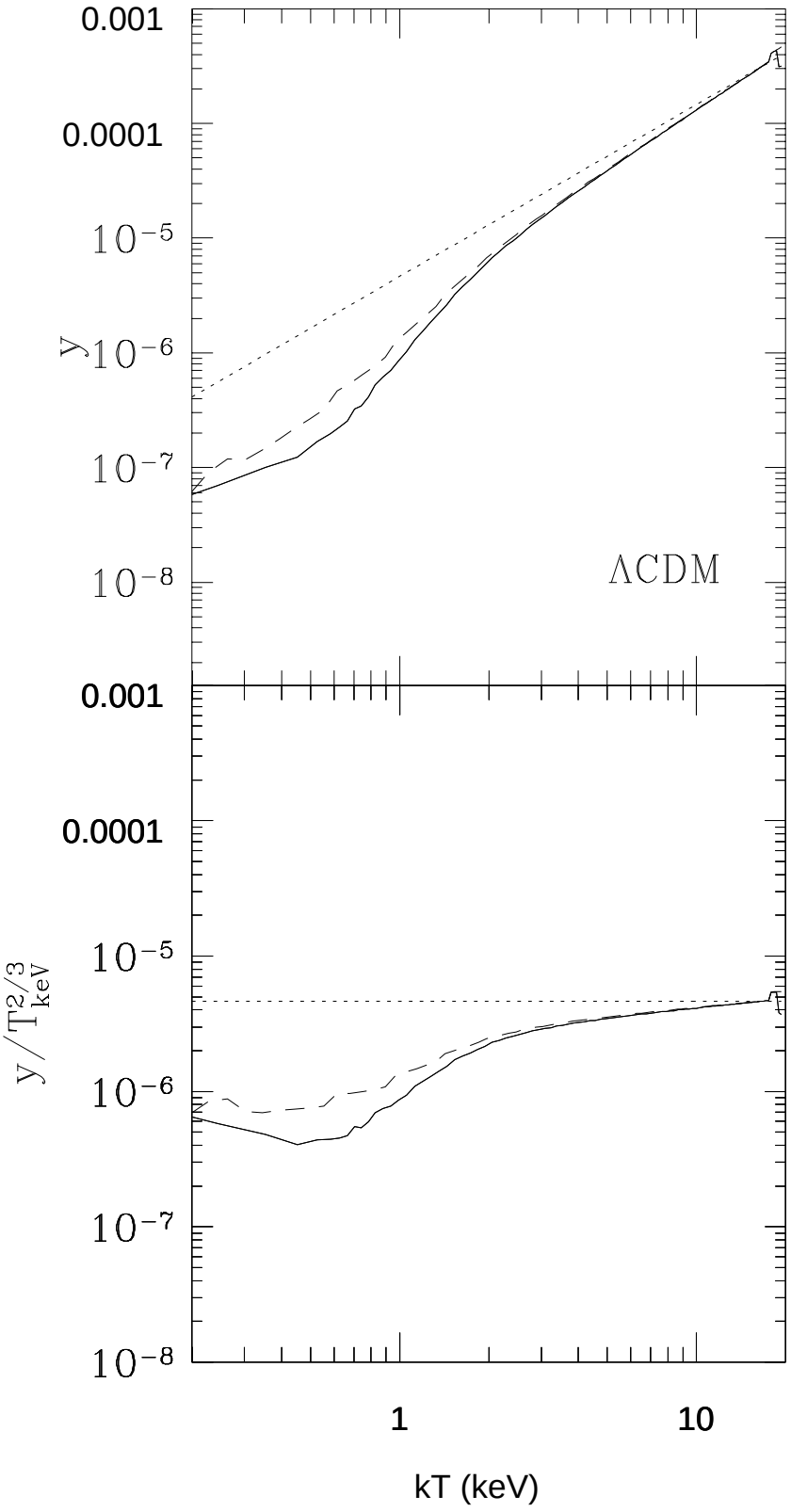
0.001
0.0001
10^{-5}
10^{-6}
10^{-7}
10^{-8}
y
ΛCDM
0.001
0.0001
10^{-5}
10^{-6}
10^{-7}
10^{-8}
$y/T^{2/3}_{keV}$
1
10
kT (keV)

Fig. 4

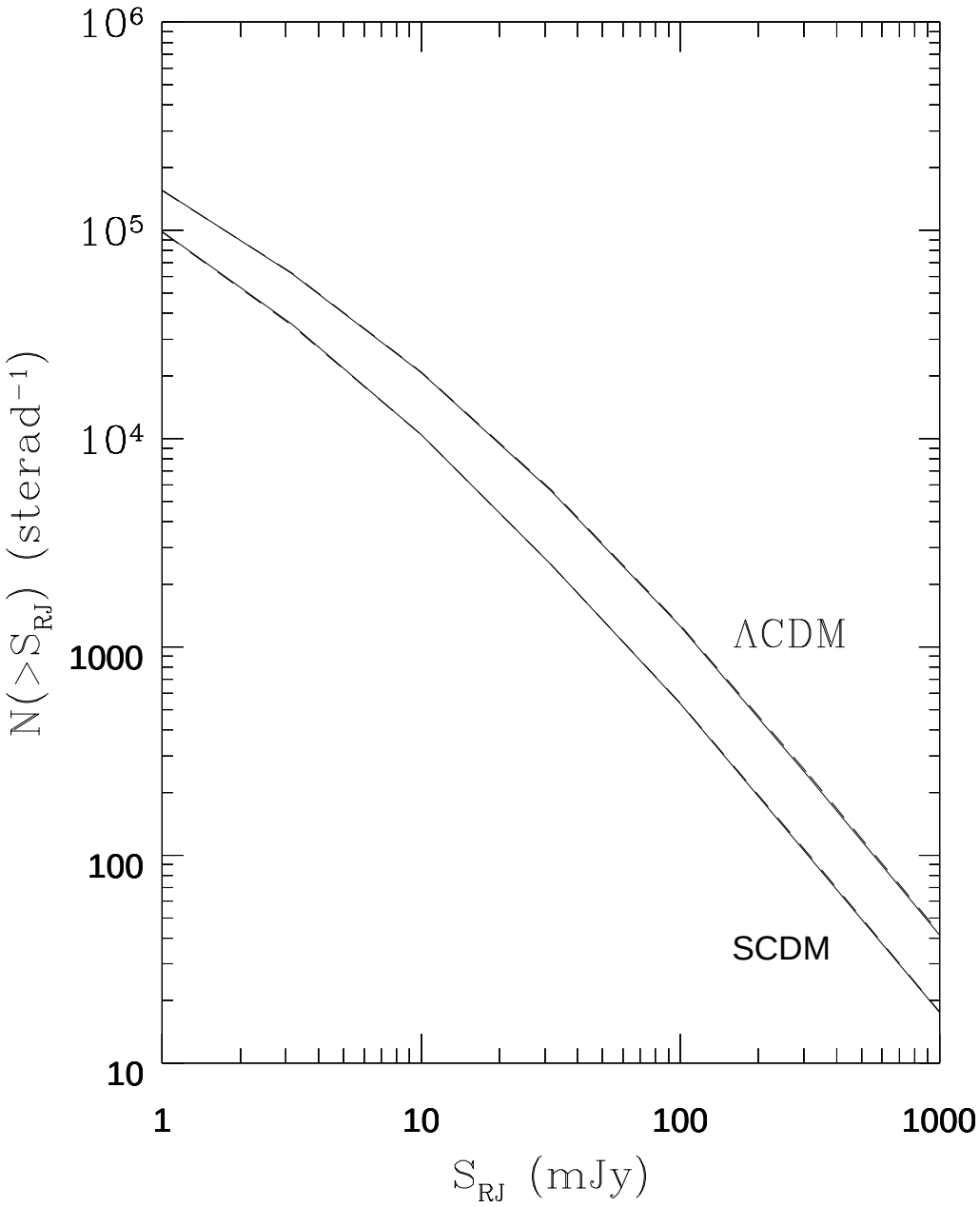
10^6
10^5
10^4
1000
100
10
$N(>S_{RJ})$ (sterad^{-1})
ΛCDM
SCDM
1
10
100
1000
S_{RJ} (mJy)

Fig.5

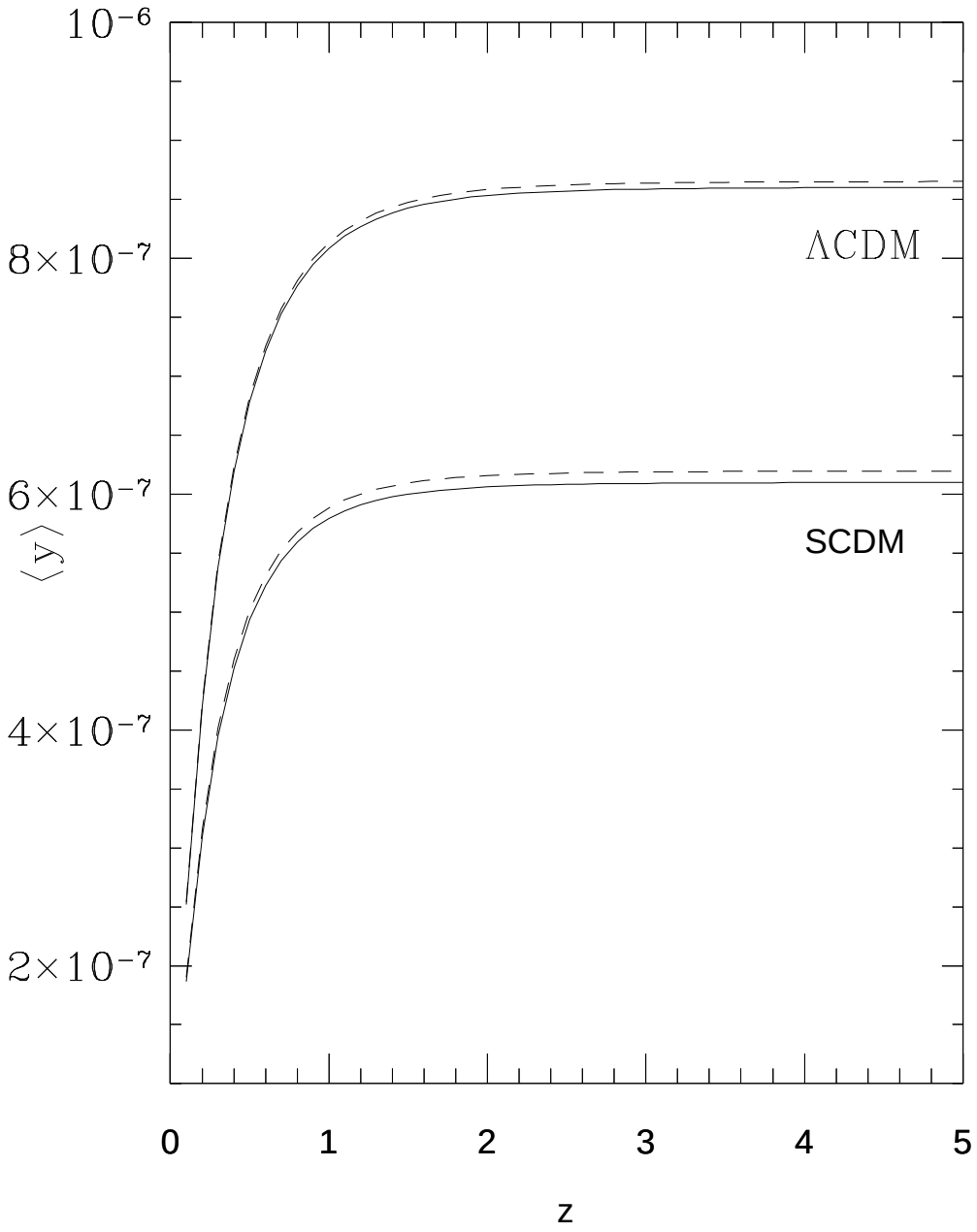
10^{-6}
8×10^{-7}
6×10^{-7}
4×10^{-7}
2×10^{-7}
$\langle y \rangle$
ΛCDM
SCDM
0
1
2
3
4
5
z

Fig. 6